Acta Mech. Sin. (2011) 27(5):668–674
DOI 10.1007/s10409-011-0483-3

RESEARCH PAPER

The influences of wall Lorentz force and field Lorentz force on the cylinder drag reduction

Hui Zhang · Bao-Chun Fan · Zhi-Hua Chen · Yan-Ling Li

Received: 18 May 2010 / Revised: 4 March 2011 / Accepted: 14 March 2011

Abstract In this paper, the effects of Lorentz force on drag reduction for a circular cylinder have been studied experimentally and numerically. Based on its effects on drag reduction, the Lorentz force is found to be classified into two parts: one acts directly on the cylinder, named as the wall Lorentz force, and the other called the field Lorentz force acts on the fluid inside the boundary layer. The wall Lorentz force leads to the generation of a thrust, whereas the field Lorentz force results in drag increase. Since the former dominates the drag variation, the drag would reduce accordingly and even turn into negative (thrust) with the application of Lorentz force.

Keywords Cylinder wake · Flow control · Lorentz force · Electromagnetic control

1 Introduction

It is well known that a flow past a bluff body may induce the undesirable vortex street behind, at the same time it may causes fluctuation in cylinder drag and lift forces, structural vibrations and acoustic noise. There are many control methods and technologies developed to suppress such phenomena [1–4]. Electromagnetic control of flow separation is considered to be one of the most practical approaches. It utilizes the generation of Lorentz forces in an electrically conducting fluid (such as seawater) to affect the fluid in the vicinity of the electromagnetic field [5–8].

So far, many investigations have been performed for electromagnetic control of the flow past a circular cylinder. Crawford and Karniadakis [9] applied direct numerical simulation to investigate the effects of Lorentz force for the control of flow separation, and their results showed that the Lorentz force could indeed eliminate the vortex shedding. Weier et al. [10] presented both experimental study and numerical calculations on active open loop control of the flow around a cylinder by means of electromagnetic forces. A circular cylindrical test body was covered with electrodes and magnets which were used to create a Lorentz force parallel to the body surface, and the suppressive effect of Lorentz force on flow separation and Karman vortex streets was confirmed. Kim et al. [11] discussed the drag reduction effect in the coverage regions of electro-magnetic actuators. Using the same method of Karniadakis', Posdziech and Grundmann [12] investigated numerically the control of seawater flows over a circular cylinder. Based on two-dimensional simulations of N-S equations in the range $10 < Re < 300$, they showed that the Lorentz force could stabilize the flow, and the cylinder drag depended strongly on the geometry of the electromagnetic actuators and their locations at the cylinder surface. In addition, both experimental and numerical investigations on the control of cylinder wake with Lorentz forces were performed by our research group, the open control, closed-loop control and optimal control methods were developed to improve its control efficiency [13–16].

However, many experimental and numerical studies were concentrated on the modified flow behavior around and behind a cylinder after the application of Lorentz force, from which a confused conclusion could sometimes be drawn, as found in some earlier publications [10,12], that the momentum gain produced by Lorentz forces in boundary layer can result in an increase of the friction and a decrease of pressure drag, and even the generation of a thrust if the Lorentz force is large enough. In fact, the applied Lorentz force can be decomposed into two parts, i.e. the field Lorentz force $F_\theta\big|_{\xi>0}$ and the wall Lorentz force $F_\theta\big|_{\xi=0}$ and their effects on the drag reduction are opposite. However, there are few studies concerning the underlying mechanism of the electromagnetic control of cylinder wake, which is related to the influ-

H. Zhang · B.-C. Fan (✉) · Z.-H. Chen · Y.-L. Li
Science and Technology on Transient Physics Laboratory,
Nanjing University of Science and Technology,
210094 Nanjing, China
e-mail: bcfan@mail.njust.edu.cn

ences involving the field Lorentz force and the wall Lorentz force.

In this paper, the influences of Lorentz force on the cylinder wake and hydrodynamic force are discussed in detail. Based on the effects on drag reduction, the applied Lorentz force can be divided into two parts: the field Lorentz force and the wall Lorentz force. The field Lorentz force affects flow behavior and results in momentum gain (or drag increase) only near the cylinder surface. On the other hand, the wall Lorentz force acts directly on the cylinder surface and results in an increase of the pressure on the cylinder leeward surface, which leads to a decrease in drag. Furthermore, a thrust or negative drag may be generated if the wall Lorentz force is large enough.

2 Experimental and numerical investigations

Experiments were performed in a weak copper sulphate ($CuSO_4$) solution with almost the same density and conductivity of seawater. Potassium permanganate ($KMnO_4$) was selected as a dark violet marker. The test cylinder with 2 cm diameter was covered with electrodes and magnets alternately. The detail description about experiments can be found in Ref. [16].

The governing equations in the exponential-polar coordinates (ξ, η) for incompressible electrically conducting fluid can be written in the dimensionless form as

$$H\frac{\partial \Omega}{\partial t} + \frac{\partial (U_r \Omega)}{\partial \xi} + \frac{\partial (U_\theta \Omega)}{\partial \eta} = \frac{2}{Re}\left(\frac{\partial^2 \Omega}{\partial \xi^2} + \frac{\partial^2 \Omega}{\partial \eta^2}\right) + NH^{1/2}\left(\frac{\partial F_\theta}{\partial \xi} + 2\pi F_\theta - \frac{\partial F_r}{\partial \eta}\right), \quad (1)$$

$$\frac{\partial^2 \psi}{\partial \xi^2} + \frac{\partial^2 \psi}{\partial \eta^2} = -H\Omega, \quad (2)$$

with initial and boundary conditions of

$$\Omega = -\frac{1}{H}\frac{\partial^2 \psi}{\partial \xi^2}, \quad \text{at } t = 0, \quad \psi = 0, \quad \text{on } \xi = 0, \quad (3)$$

$$\psi = -2\mathrm{sh}(2\pi\xi)\sin(2\pi\eta), \quad \Omega = 0, \quad \text{on } \xi > 0, \quad (4)$$

$$\Omega = -\frac{1}{H}\frac{\partial^2 \psi}{\partial \xi^2}, \quad \text{at } t > 0, \quad \psi = 0, \quad \text{on } \xi = 0, \quad (5)$$

$$\psi = -2\mathrm{sh}(2\pi\xi)\sin(2\pi\eta), \quad \Omega = 0, \quad \text{on } \xi = \xi_\infty, \quad (6)$$

where $r = \mathrm{e}^{2\pi\xi}$ and $\theta = 2\pi\eta$, r and θ are polar coordinates. The stream function ψ is defined as $\partial\psi/\partial\eta = U_r = H^{1/2}u_r$, $-\partial\psi/\partial\xi = U_\theta = H^{1/2}u_\theta$, while the vorticity Ω is defined as $\Omega = (\partial U_\theta/\partial\xi - \partial U_r/\partial\eta)/H$, with u_r and u_θ are the velocity components in r and θ directions, respectively. Furthermore, $H = 4\pi^2\mathrm{e}^{4\pi\xi}$, $Re = 2u_\infty a/\nu$, u_∞ is the free-stream velocity, ν is the kinematic viscosity, a is the cylinder radius, the non-dimensional time is $t = t^* u_\infty/a$. The interaction parameter is defined as $N = j_0 B_0 a/(\rho u_\infty^2)$, with current density $j_0 = \sigma E_0$, where σ is the electric conductivity, E_0 the electric field and B_0 the magnetic field. Lorentz force $\boldsymbol{F}$ can be described by a distributed function given by Weier et al. [10] , when it is applied locally on the cylinder in the range of θ_0 to $\theta_0 + \Delta\theta$ from the stagnation point along the cylinder circumference in both the clockwise and counterclockwise directions, then

$$F_r = 0,$$

$$F_\theta = \mathrm{e}^{-\alpha(r-1)} g(\theta),$$

with

$$g(\theta) = \begin{cases} 1, & \theta_0 \le \theta \le \theta_0 + \Delta\theta, \\ -1, & 360^\circ - (\theta_0 + \Delta\theta) \le \theta \le 360^\circ - \theta_0, \\ 0, & \text{elsewhere}, \end{cases} \quad (7)$$

where α is constant, refering to the penetration intensity of Lorentz force in the fluid.

Based on Eqs. (1)–(6), it is obvious that the Lorentz force on the wall denoted by $F_\theta\big|_{\xi=0}$ does not have any effect on the stream function/vorticity fields due to non-slip boundary, and the velocity field is also independent of $F_\theta\big|_{\xi=0}$ consequently. Namely, the stream function/vorticity and velocity fields are affected only by the field Lorentz force $F_\theta\big|_{\xi>0}$. This conclusion can also be further verified by numerical calculations.

3 Hydrodynamic force

A net hydrodynamic force F^θ will be exerted on a circular cylinder immersed in a fluid, which can be defined in the dimensionless form as

$$C_\mathrm{F}^\theta = \frac{2F^\theta}{\rho u_\infty^2} = \sqrt{\left(\frac{2F_\tau^\theta}{\rho u_\infty^2}\right)^2 + \left(\frac{2F_\mathrm{p}^\theta}{\rho u_\infty^2}\right)^2} = \sqrt{(C_\tau^\theta)^2 + (C_\mathrm{p}^\theta)^2}, \quad (8)$$

where the shear stress C_τ^θ generated from the velocity gradient on the boundary is expressed as

$$C_\tau^\theta = \frac{2F_\tau^\theta}{\rho u_\infty^2} = \frac{2\mu}{\rho u_\infty^2}\frac{\partial u_\theta}{\partial r} = \frac{4}{Re}\Omega, \quad (9)$$

and the pressure coefficient at Point θ on the surface of the cylinder can be calculated from its definition [17]

$$C_\mathrm{p}^\theta = \frac{2F_\mathrm{p}^\theta}{\rho u_\infty^2} = \frac{2(p_\theta - p_\infty)}{\rho u_\infty^2} = P_\theta - P_\infty, \quad (10)$$

where the dimensionless pressure is $P = 2p/(\rho u_\infty^2)$ with p being pressure in the flow field. Then, C_p^θ can be formulated further by the following mathematical derivation.

The momentum equations with the source of Lorentz force are

$$\frac{\partial P}{\partial \xi} = -4\pi\mathrm{e}^{2\pi\xi}\frac{\partial u_r}{\partial t} - 2u_r\frac{\partial u_r}{\partial \xi} - 2u_\theta\frac{\partial u_r}{\partial \eta} + 4\pi u_\theta^2 - \frac{4}{Re}\frac{\partial \Omega}{\partial \eta}, \quad (11)$$

$$\frac{\partial P}{\partial \eta} = -4\pi\mathrm{e}^{2\pi\xi}\frac{\partial u_\theta}{\partial t} - 2u_r\frac{\partial u_\theta}{\partial \xi} - 2u_\theta\frac{\partial u_\theta}{\partial \eta}$$

$$+4\pi u_r u_\theta + \frac{4}{Re}\frac{\partial \Omega}{\partial \xi} + 4\pi N F_\theta. \quad (12)$$

On the surface of the cylinder $\boldsymbol{u} = \boldsymbol{0}$, one obtains

$$\left(\frac{\partial P}{\partial \xi} = -\frac{4}{Re}\frac{\partial \Omega}{\partial \eta}\right)_{\xi=0}, \quad (13)$$

$$\left(\frac{\partial P}{\partial \eta} = \frac{4}{Re}\frac{\partial \Omega}{\partial \xi} + 4\pi N F_\theta\right)_{\xi=0}. \quad (14)$$

Integrating Eq. (14) in the η direction from $\eta = 0$ to η, one obtains

$$P_\theta - P_0 = \frac{4}{Re}\int_0^\eta \frac{\partial \Omega}{\partial \xi}\mathrm{d}\eta + 4\pi N \int_0^\eta F_\theta\big|_{\xi=0}\mathrm{d}\eta. \quad (15)$$

Integrating Eq. (11) in the ξ direction from $\xi = 0$ to ξ, one obtains

$$P_\infty - P_0 = -4\pi \int_0^\infty \frac{\partial u_r}{\partial t}\mathrm{e}^{2\pi\xi}\mathrm{d}\xi - 1 - 2\int_0^\infty u_\theta \frac{\partial u_r}{\partial \eta}\mathrm{d}\xi + 4\pi \int_0^\infty u_\theta^2 \mathrm{d}\xi - \frac{4}{Re}\int_0^\infty \frac{\partial \Omega}{\partial \eta}\mathrm{d}\xi. \quad (16)$$

Then

$$C_\mathrm{p}^\theta = P_\theta - P_\infty = C_\mathrm{pF}^\theta + C_\mathrm{pL}^\theta, \quad (17)$$

where

$$C_\mathrm{pF}^\theta = \frac{4}{Re}\int_0^\eta \frac{\partial \Omega}{\partial \xi}\mathrm{d}\eta + C_\mathrm{p}^0, \quad (18)$$

$$C_\mathrm{p}^0 = 1 + 4\pi \int_0^\infty \frac{\partial u_r}{\partial t}\mathrm{e}^{2\pi\xi}\mathrm{d}\xi + 2\int_0^\infty u_\theta \frac{\partial u_r}{\partial \eta}\mathrm{d}\xi - 4\pi \int_0^\infty u_\theta^2 \mathrm{d}\xi + \frac{4}{Re}\int_0^\infty \frac{\partial \Omega}{\partial \eta}\mathrm{d}\xi, \quad (19)$$

$$C_\mathrm{pL}^\theta = 4\pi N \int_0^\eta F_\theta\big|_{\xi=0}\mathrm{d}\eta. \quad (20)$$

Therefore, the pressure gradient in flow fields is affected by the field Lorentz force $F_\theta\big|_{\xi>0}$, whereas the pressure and its gradient on the wall are affected by both the field and the wall Lorentz force. Subscript "F" represents the wall pressure induced by the field Lorentz force and "L" denotes the wall pressure induced by the wall Lorentz force.

The hydrodynamic force can also be regarded as consisting of a drag force and a lift force, which denote the force components in the streamwise and the normal directions, respectively. The distribution of drag force, consisting of pressure drag $C_\mathrm{p}^\theta \cos\theta$ and friction drag $C_\tau^\theta \sin\theta$, is expressed as

$$C_\mathrm{d}^\theta = C_\mathrm{p}^\theta \cos\theta + C_\tau^\theta \sin\theta = C_\mathrm{dF}^\theta + C_\mathrm{dL}^\theta, \quad (21)$$

where

$$C_\mathrm{dF}^\theta = C_\mathrm{pF}^\theta \cos\theta + C_\tau^\theta \sin\theta, \quad (22)$$

$$C_\mathrm{dL}^\theta = C_\mathrm{pL}^\theta \cos\theta = 4\pi N \cos\theta \int_0^\eta F_\theta\big|_{\xi=0}\mathrm{d}\eta. \quad (23)$$

The total force is obtained by integrating the force distribution function along the cylinder surface, by defining the dimensionless form of

$$C = \frac{F}{\rho u_\infty^2 a},$$

and we can then write

$$C_\mathrm{d} = \int_0^{2\pi} C_\mathrm{d}^\theta \mathrm{d}\theta = C_\mathrm{dF} + C_\mathrm{dL}, \quad (24)$$

where

$$C_\mathrm{dF} = \frac{2}{Re}\int_0^1 \left(2\pi\Omega - \frac{\partial \Omega}{\partial \xi}\right)\sin(2\pi\eta)\mathrm{d}\eta, \quad (25)$$

$$C_\mathrm{dL} = -2\pi N \int_0^1 F_\theta\big|_{\xi=0}\sin(2\pi\eta)\mathrm{d}\eta. \quad (26)$$

The numerical method consists of an alternating-direction-implicit (ADI) algorithm for the vorticity transport equation and fast Fourier transforms (FFT) for the Poisson equation with a second-order accuracy. Details of the numerical simulation can be found in Refs. [13–16]. Numerical results here are obtained at $Re = 150$ with computational step sizes of $\Delta\xi = 0.004$, $\Delta\eta = 0.002$ and $\Delta t = 0.005$. The slots at the front and rear stagnation points are not electrodes but rather the location of $\theta_0 = 5°$ and $\Delta\theta = 170°$, with the step of 10°.

4 Results and discussions

With the control of Lorentz force acting parallel to the cylinder surface in the flow direction, the fluid in the boundary layer is accelerated to overcome the adverse pressure gradient, which leads to the suppression of flow separation.

Figure 1 shows the cylinder wake flow under different Lorentz forces (N). Figure 1a represents the experimental results, while Fig. 1b is the corresponding numerical results. Without Lorentz force, $N = 0$, the flow is unsteady and shows the characteristic features of Karman vortex street. For a small Lorentz force, $N = 0.7$, an interesting modification of flow characteristics can be observed. Although the flow is unsteady, the flow separation region is diminished. With a further increase of Lorentz force, $N = 2$, the separation points disappear and the flow becomes stable.

4.1 Influences of field Lorentz force on the force at cylinder surface

4.1.1 Shear stress distribution at the cylinder surface

Based on the calculated results for $Re = 150$, with the action of different Lorentz forces, the distributions of shear stresses (C_τ^θ) at the cylinder surface at the reference time of T_0 at which the lift is zero are shown in Fig. 2. From Eq. (9), C_τ^θ is proportional to the vorticity on the cylinder surface. Thus, the absolute value of the shear stress increases with an increase of the Lorentz force (Fig. 2).

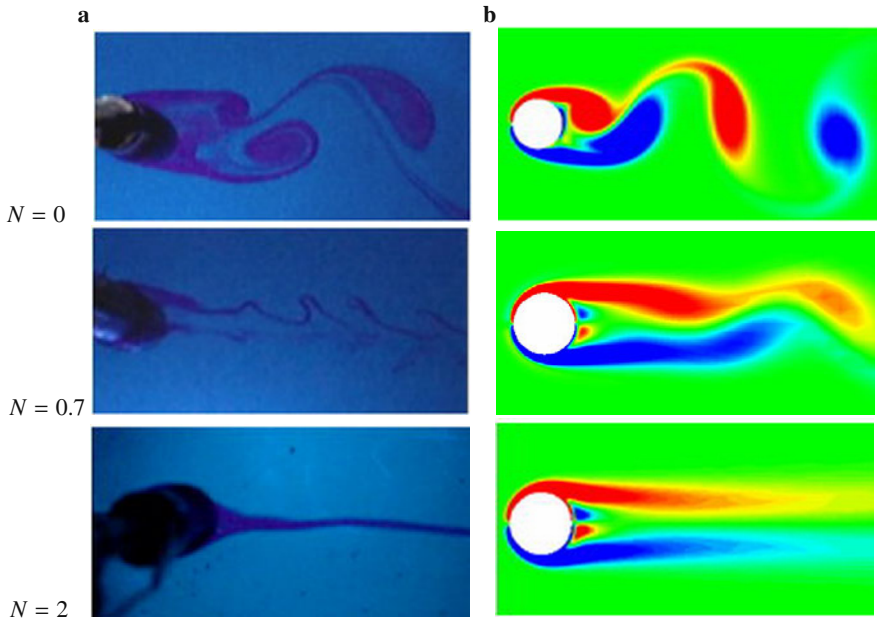

Fig. 1 Cylinder wake flow under different Lorentz forces. **a** Experiments; **b** Calculations

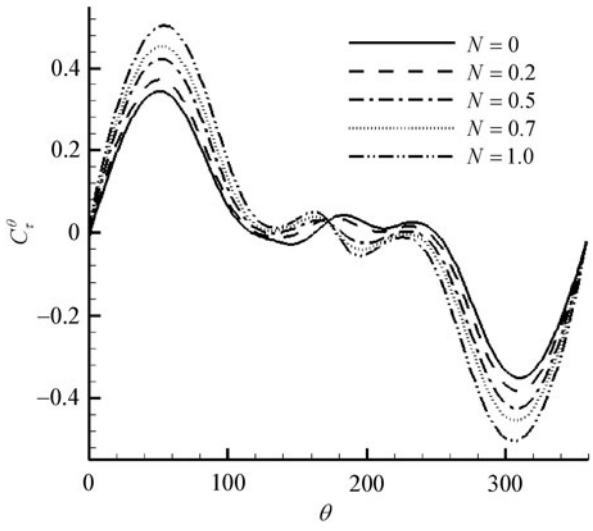

Fig. 2 Distribution of friction C_τ^θ versus different field Lorentz forces at time T_0

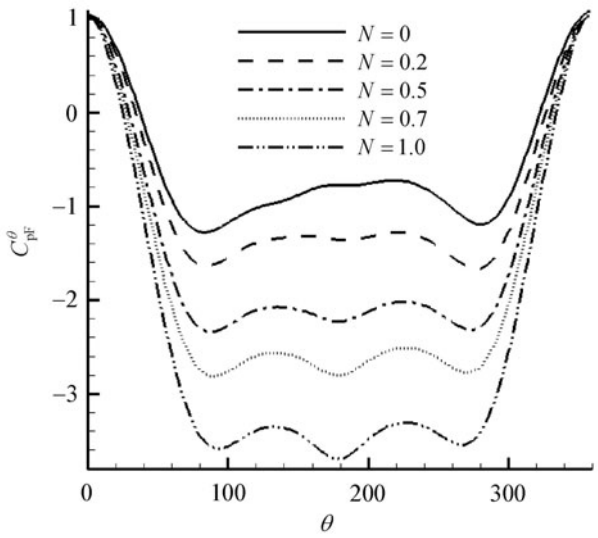

Fig. 3 Variations of C_{pF}^θ under the action of field Lorentz force at time T_0

4.1.2 The pressure distribution at the cylinder surface

The pressure at the cylinder surface is composed of two components, C_{pF}^θ and C_{pL}^θ, where C_{pF}^θ is generated by the flow field, and C_{pL}^θ is generated by the wall Lorentz force. With the application of Lorentz forces, the distributions of C_{pF}^θ at time T_0 are shown in Fig. 3. The flow acceleration in the front part of the cylinder results in a decrease of pressure on the cylinder surface. Therefore, the curves of C_{pF}^θ move downward under the action of Lorentz force, and the pressure reduction increases with an increase of Lorentz force.

4.1.3 The drag distribution of the cylinder

According to Eq. (21), the distribution of drag on the cylinder surface, C_{d}^θ, consists of C_{dF}^θ and C_{dL}^θ which are generated by the flow field and the wall Lorentz force, respectively.

C_{dF}^θ is equal to the sum of C_τ^θ and C_{pF}^θ projecting in the inflow direction as described by Eq. (22). Figure 4 shows the distribution of C_{dF}^θ along the cylinder surface under different Lorentz forces at time T_0. With an increase of Lorentz force, C_{dF}^θ decreases on the windward surface, but increases on the leeward surface. Since the total drag force C_{dF} ob-

tained by integrating C_{dF}^{θ} along the whole cylinder surface is dominated by C_{dF}^{θ} on the leeward surface, C_{dF} increases with an increase of Lorentz force. Therefore, the field Lorentz force increases the drag of cylinder.

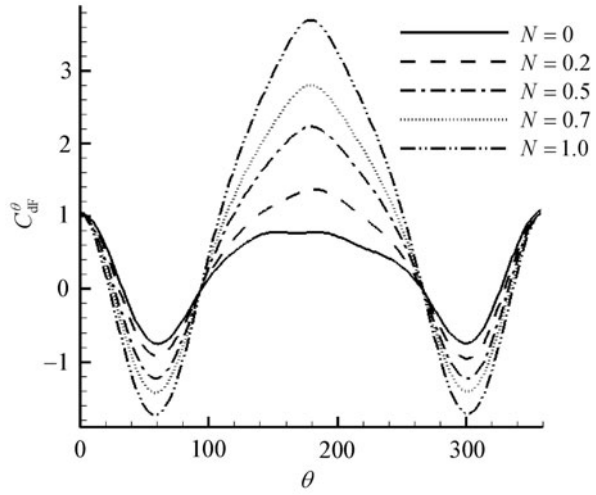

Fig. 4 Distributions of C_{dF}^{θ} with different Lorentz force at time T_0

4.2 Influences of wall Lorentz force on the force at cylinder surface

4.2.1 The pressure distribution at cylinder surface

The pressure at the cylinder surface affected by the wall Lorentz force is denoted by C_{pL}^{θ}. Figure 5 displays the distributions of C_{pL}^{θ} with different Lorentz forces. All curves are positive and symmetrical about the line of $\theta = 180°$, and it is clear that C_{pL}^{θ} increases with an increase of Lorentz force and reaches its maximum value at $\theta = 180°$.

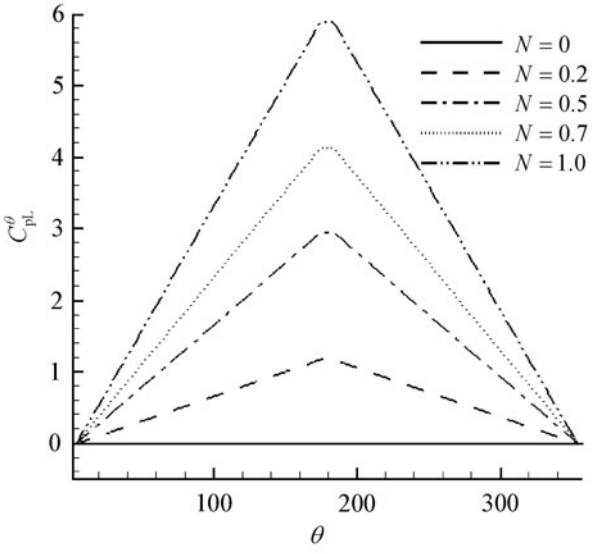

Fig. 5 Distributions of pressure coefficient C_{pL}^{θ} with different Lorentz force

4.2.2 The drag distribution of the cylinder

The drag generated by the wall Lorentz force, denoted by C_{dL}^{θ}, is dependent directly on C_{pL}^{θ} (Eq. (23)). The distributions of C_{dL}^{θ} with different Lorentz forces are shown in Fig. 6. It is obvious that C_{dL}^{θ} is positive on the windward and negative on the leeward surfaces, and their absolute values also increase with an increase of Lorentz force. In addition, the signs of C_{dL}^{θ} in Fig. 6 are opposite to the signs of C_{dF}^{θ} in Fig. 4 on the leeward surface, and its absolute value is far higher on the leeward than that on the windward surfaces. Therefore, C_{dL} is dominated by C_{dL}^{θ} on the leeward surface, and is thus always negative, which means that the wall Lorentz force always generates thrust. Moreover, the thrust increases with an increase of Lorentz force.

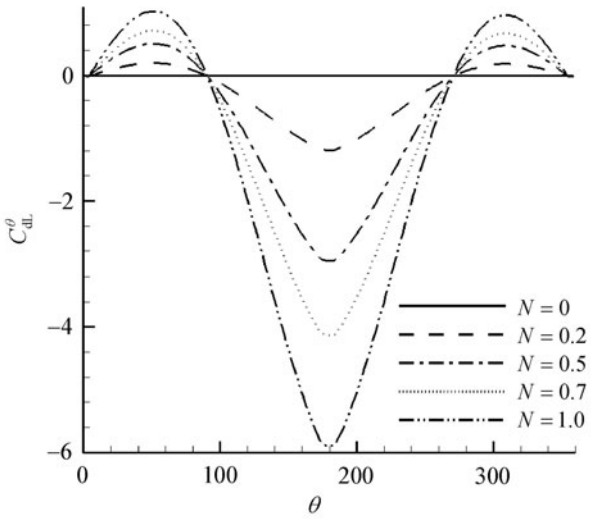

Fig. 6 Distributions of C_{dL}^{θ} with different Lorentz force

In order to validate the effect of wall Lorentz force experimentally, the cylinder is inserted into a still fluid. After the activation of the actuators, the strain gage is bent in the flow direction under the action of thrust generated by the Lorentz force, where the flow near the cylinder surface induced by the Lorentz force is negligible. As shown in Fig. 7, the output signal increases rapidly and turns to be relative stable with the Lorentz force turned on, whereas it decreases dramatically as the Lorentz force is turned off.

4.3 Drag reduction under the action of Lorentz force

The total drag force C_{d} is the sum of the drag forces caused by the field, C_{dF}, and the wall Lorentz force, C_{dL}. Figure 8 shows the variations of C_{d}, C_{dF} and C_{dL} versus Lorentz forces. It can be seen that C_{dF} increases with an increase of Lorentz force, however, it is contrary for C_{dL}. In addition, the increasing rate of C_{dF} is lower than the decreasing rate of C_{dL}. Therefore, the total drag C_{d} is dominated by C_{dL},

and decreases accordingly. The negative value of C_d denotes the fact that the total drag force of the cylinder has turned into a net thrust, which also means that the direct propulsion of wall Lorentz force (C_{dL}) has overcome the cylinder drag caused by the flow field (C_{dF}).

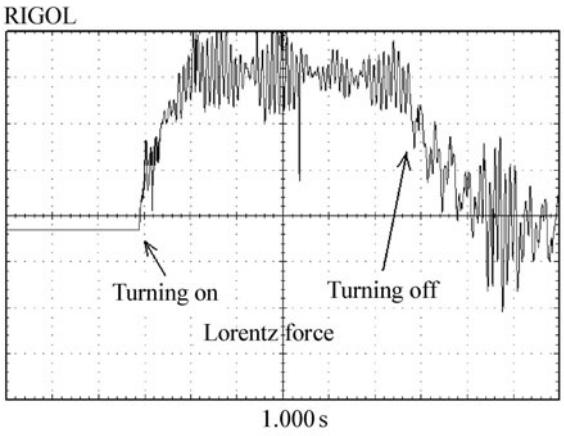

Fig. 7 Experimental results of the thrust under the wall Lorentz force

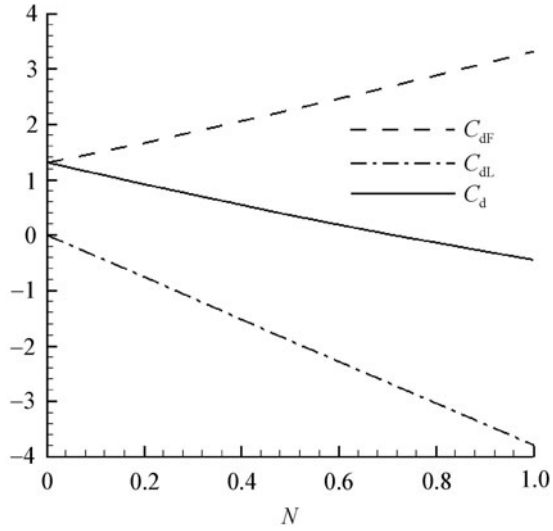

Fig. 8 Variations of C_d, C_{dF} and C_{dL} with Lorentz forces

Figure 9 shows experimental results of the evolution of drag. With the Lorentz force turned on, the drag decreases, which describes the same modification tendency as given by numerical results mentioned above.

5 Conclusions

The effects of Lorentz force on a circular cylinder drag reduction have been studied both experimentally and numerically. The Lorentz force can be classified into the field

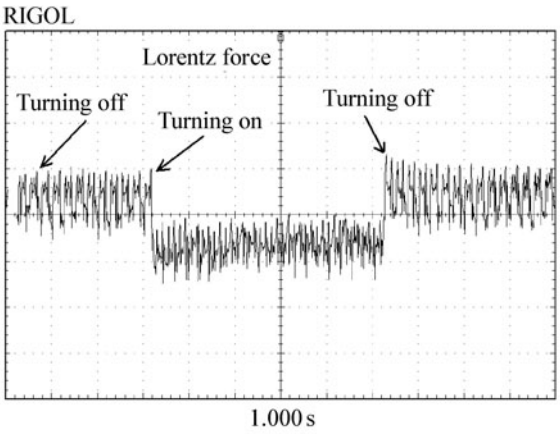

Fig. 9 Experimental results of the evolution of drag under the Lorentz force

Lorentz force and the wall Lorentz force, which have opposite effects on the drag reduction. The field Lorentz force can accelerate the fluid in the boundary layer, which increases the difference between the pressures on the windward and leeward sufaces, consequently increases the pressure drag. On the other hand, the wall Lorentz force increases the pressure on the wall monotonically from its front to the back stagnation point, which decreases the difference between the pressures on the windward and the leeward surfaces, therefore leads to the generation of a thrust. The total drag of the cylinder is dominated by the wall Lorentz force, and thus it would decrease, and may even become negative (thrust) if the Lorentz force is large enough.

References

1 Henoch, C., State, J.: Experimental investigation of a salt water turbulent boundary layer modified by an applied streamwise magnetohydrodynamic body force. Physics of Fluids **7**(6), 1371–1383 (1995)

2 Wu, C.J., Wang, L., Wu, J.Z.: Suppression of the von Karman vortex street behind a circular cylinder by a traveling wave generated by a flexible surface. Journal of Fluid Mechanics **574**, 365–391 (2007)

3 Tang, S., Aubry, N.: On the symmetry breaking instability leading to vortex shedding. Physics of Fluids **9**(9), 2550–2561 (1997)

4 Roussopoulos, K.: Feedback control of vortex shedding at low Reynolds numbers. Journal of Fluid Mechanics **248**, 267–296 (1993)

5 Breuer, K.S., Park, J., Henoch, C.: Actuation and control of a turbulent channel flow using Lorentz forces. Physics of Fluids **16**(4), 897–907 (2004)

6 Berger, T., Kim, J., Lee, C., et al.: Turbulence boundary layer control utilizing the Lorentz force. Physics of Fluids **12**(3), 631–649 (2000)

7 Mutschke, G., Gerbeth, G., Albrecht, T., et al.: Separation control at hydrofoils using Lorentz forces. European Journal of

Mechanics-B/Fluids **25**(2),137–152 (2006)
8 Braun, E.M., Lu, F.K., Wilson, D.R.: Experimental research in aerodynamic control with electric and electromagnetic fields. Progress in Aerospace Sciences **45**(1), 30–49 (2009)
9 Crawford, C.H., Karniadakis, G.E.: Control of external flows via electro-magnetic fields. AIAA-952185 (1995)
10 Weier, T., Gerbeth, G., Mutschke, G., et al.: Experiments on cylinder wake stabilization in an electrolyte solution by means of electromagnetic forces localized on the cylinder surface. Experimental Thermal and Fluid Science **16**(1), 84–91 (1998)
11 Kim, S., Lee, C.M.: Control of flows around a circular cylinder: suppression of oscillatory lift force. Fluid Dynamics Research **29**(1), 47–63 (2001)
12 Posdziech, O., Grundmann, R.: Electromagnetic control of seawater flow around circular cylinders. European Journal of Mechanics-B/Fluids **20**(2), 255–274 (2001)
13 Chen, Z.H., Fan, B.C.: Numerical investigation on wake of cylinder covered with electro-magnetic actuator. Acta Mechanica Sinica **34**(6), 978–983 (2002) (in Chinese)
14 Zhang, H., Fan, B.C., Chen, Z.H.: Optimal control of cylinder wake by electromagnetic force based on the adjoint flow field. European Journal of Mechanics-B/Fluids **29**(1), 53–60 (2010)
15 Zhang, H., Fan, B.C., Chen, Z.H.: Control approaches for a cylinder wake by electromagnetic force. Fluid Dynamics Research **41**(4), 045507 (2009)
16 Zhang, H., Fan, B.C., Chen, Z.H. et al.: Suppression of flow separation around a circular cylinder by utilizing Lorentz force, China Ocean Engineering **22**(1), 87–95 (2008)
17 Chen, Z.H.: Electro-magnetic control of cylinder wake. [Ph.D. Thesis], New Jersey Institute of Technology, Newark, NJ (2001)